Journal of Applied Polymer Science

Synthesis and Surface Characterization of Copoly(imide alkyl ether)s Containing Pendant Fluoroalkyl Groups

Christopher J. Wohl,[1] Leanna L. Foster,[2] Samantha I. Applin,[2] John W. Connell[1]
[1]NASA Langley Research Center, Hampton, Virginia 23681
[2]NASA Langley Research Summer Scholars (LARSS), NASA Langley Research Center, Hampton, Virginia 23681
Correspondence to: C. Wohl (E-mail: c.j.wohl@nasa.gov)

ABSTRACT: A series of copoly(imide alkyl ether)s were synthesized to explore surface migration of fluorinated alkyl ether blocks (AEFO)s. Mechanical and surface properties of solution cast, thermally imidized films were determined. Incorporation of the AEFO oligomers at loading levels up to 5 wt % resulted in a slight decrease (usually less than 10%) in tensile modulus. Surface migration of the AEFOs raised the advancing water contact angle from approximately 80° to above 95° for the copolymer systems. The composition at which addition of more AEFO further increased water contact angle values was related to the number of fluorine atoms in the perfluorinated side chains. Surface excess concentration of the AEFO at different loading levels was calculated from X-ray photoelectron spectroscopy results. At higher AEFO loading levels, the surface excess concentration was relatively constant suggesting formation of stable structures within the bulk similar to micelle formation in surfactant solutions. Based on these results, it was determined that surface saturation occurred with the fluorinated AEFO species at loading levels as low as 1 wt % engendering changes in surface properties while retaining the bulk imide properties. © 2014 Wiley Periodicals, Inc. J. Appl. Polym. Sci. **2015**, *132*, 41538.

KEYWORDS: coatings; monomers; oligomers and telechelics; structure–property relations; surfaces and interfaces

Received 8 August 2014; accepted 19 September 2014
DOI: 10.1002/app.41538

INTRODUCTION

Surface chemistry of polymeric substrates can be modified through a variety of techniques. Chemical or physical vapor deposition, self-assembled monolayers, surface-confined chemical reactions, and polymer brush growth are all effective methods to alter surface chemistry. All of these approaches require modification to an existing substrate and thus, require at least two steps, substrate generation and surface modification. Incorporation of a surface migrating agent (SMA) into the substrate during its fabrication reduces this complexity. SMAs are thermodynamically drawn to the substrate surface enabling controlled surface chemical modification with minimal SMA incorporation (Scheme 1);[1] loading levels requisite to achieve surface chemical loading limits are less than 1% (w/w).[2] In addition, this directed surface modification may result in retention of the bulk material's mechanical, thermal, and electrical properties.

Among the variety of chemical moieties that have been demonstrated to migrate to the surface in an uncured or solvated polymeric matrix, silanated, and fluorinated species are often investigated due to the significant changes in liquid wettability arising from their surface population. Small molecule, macromolecule [polyhedral oligomeric silsesquioxane (POSS)], and oligomeric silanated species have all been demonstrated to migrate to polymeric surfaces resulting in changes to liquid wettability and useful changes in surface reactivity.[3–5] Fluorinated species exhibit an even greater propensity for surface migration than silanated functionalities and have been demonstrated to undergo surface migration within a variety of matrices including polyester,[6] polyurethane,[7–9] polyacrylate,[10] and polydimethyl siloxane (PDMS) matrices,[2] among others.

Fluorine-containing, oxetane-derived SMAs have been investigated due to the relative ease of synthesis of narrow molecular weight oligomers.[11,12] In addition, these materials enable generation of polytetrafluoroethylene-like surfaces without the use of long chain perfluorinated aliphatic species which are known to generate harmful bioaccumulating perfluorinated acid species upon degradation.[13,14] Using the surface migration behavior of fluorinated groups, Wynne et al. were able to concentrate a non-fluorinated side chain functionality (—CH_2Br) at a surface by incorporating it into a fluorine-containing oxetane-derived alkyl ether.[15] The in-water wettability of a urethane system built with an oxetane-derived oligomer that had both hydrophobic and hydrophilic side chains was found to be controlled by hydrophobic surface domains.[16] Similarly, the in-water wettability of an SMA-containing urethane was decreased by

Additional Supporting Information may be found in the online version of this article.

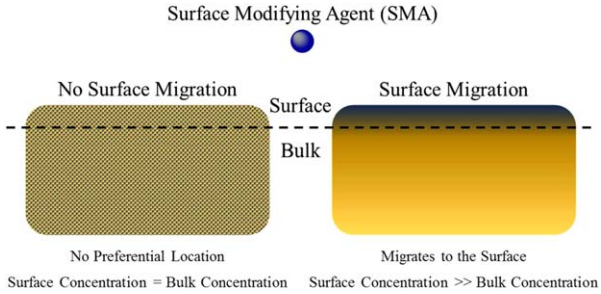

Scheme 1. Concentration variation of surface modifying agents. [Color figure can be viewed in the online issue, which is available at wileyonlinelibrary.com.]

surface concentrating a metastable hydrogen bonding moiety, which exposed hydrophobic moieties to the surface in the wetted state.[17] In fact, the propensity for these short fluorinated side chain oligomers to populate the surface is so strong that antimicrobial functionalities have been chaperoned to the surface—a novel approach toward contact biocides.[15] One reason that these fluorinated moieties can so readily populate the surface is the flexibility of the poly(oxyethylene) backbone. Alkyl ether thin films have been demonstrated to enable orientation of long paracrystalline fluorinated side chains.[18] Interestingly, the lowest surface energy for these films was determined to be at 70 mol % fluorinated monomeric units. This surface orientation was also determined to cause unusually low surface tension values for water-soluble fluorinated oxetane-derived polymers solutions.[19]

As part of our efforts to engineer materials' surfaces that exhibit abhesive, i.e., non-adhesive, interactions for a variety of future NASA missions, copoly(imide alkyl ethers)s containing pendant perfluoro groups were synthesized and characterized. This approach was designed to take advantage of the inherent properties of the two copolymer components, namely the high thermal stability, mechanical strength, and radiation resistance of polyimides,[20] and the surface migrating characteristics of oxetane-derived alkyl ethers that contain pendant perfluoro groups. These materials could minimize surface adhesion of species such as ice and insect residue on future aircraft, and Lunar or Martian dust on future exploration missions. For example, NASA is currently conducting research under the environmentally responsible aviation (ERA) program to reduce fuel consumption and engine emissions.[21] One approach which has shown potential to reduce fuel consumption is to utilize laminar flow in future aircraft designs. Contamination by particles and debris such as insect residue can disrupt laminar flow and increase drag.[22–24] In this work, the synthesis of copolymers is described, including the end-group functionalization of the oxetane-derived alkyl ether oligomers with a primary amine to enable subsequent reaction into the imide backbone. The surface migration behavior of the alkyl ethers containing pendant perfluoro groups in the copolymers was investigated using contact angle goniometry (CAG) and X-ray photoelectron spectroscopy (XPS). The Lunar dust simulant adhesion properties and surface mechanical properties will be discussed in a future publication.

EXPERIMENTAL

Materials and Methods

The hydroxyl-terminated alkyl ether containing pendant fluorinated groups (AEFO) with trade names PF636, PF656, PF154N, PF6320, and PF7002 were purchased from Omnova and used as received except for PF154N. This AEFO was purchased as an aqueous solution and was purified by azeotropic distillation of the water in toluene followed by rotary evaporation of the toluene to yield a white powder. For this work, the AEFOs will be identified by the number of fluorine atoms per oligomer (Table I). For example, PF636 has a single fluorinated methyl group in each repeat unit and, according to the manufacturer, there are an average of six repeat units per oligomer. Thus, PF636 in this work will be referred to as F_{18}. 3,3′,4,4′-Biphenyl tetracarboxylic dianhydride (s-BPDA, ChrisKev Company, $T_m = 292°C$) was refluxed in a 3 : 1 ratio of acetic acid : acetic anhydride, purified by filtration, and vacuum drying at 120°C for 6 h. 4,4′-Oxydianiline (4,4′-ODA, Wakayama Seika Kogya, $T_m = 188°C$) was used as received. All other reactants and solvents were used as received. Proton and carbon nuclear magnetic resonance (^1H and ^{13}C NMR) spectra were recorded on a Bruker (Avance 300) Multinuclear Spectrometer operating at 300.152 MHz and 75.468 MHz, respectively. All spectra were collected in $CDCl_3$ and the determined chemical shifts were relative to tetramethyl silane (TMS) at $\delta = 0$ PPM. Polymer film mechanical properties were determined on a Sintech 2W test frame with a crosshead speed of 5.08 mm/min at ambient temperature according to ASTM D882-09. The data were collected and analyzed using Testworks 8.0. Water contact angle data were collected using a First Ten Angstroms FTA 1000B contact angle goniometer. Tilting axis contact angles were measured for each sample using an 8 μL water droplet. Interfacial tension measurements of a suspended water drop were made before experimentation to verify water purity and precision of the focused image. Contact angles were determined by drop shape analysis from a series of images collected at a rate of 2 frames/s. A minimum of three measurements were recorded for each sample. XPS measurements were collected on a ThermoFisher ESCAlab 250 X-ray photoelectron spectrometer. The high resolution XPS data was deconvoluted via a minimalist approach using the fewest Gaussian peaks to recreate line shapes.

Synthesis of Nitro-Terminated AEFOs

The synthesis was adapted from a similar synthetic procedure involving a poly(propylene glycol).[25] As an example, a three-necked round-bottomed flask was charged with the hydroxyl-terminated AEFO oligomer (F_{40}) 61.17 g, 0.0366 mol) and toluene (125 mL). Triethylamine (41 mL, 29 g, 0.29 mol) was added to this solution

Table I. AEFO Oligomer Molecular Weights Determined by ^1H NMR End Group Analysis

AEFO	Designation	OH-terminated (g/mol)[a]	NO_2-terminated (g/mol)	NH_2-terminated (g/mol)
PF636	F_{18}	1150	1450	1310
PF656	F_{30}	1490	1570	1530
PF154N	F_{30B}	3464	3060	3200
PF7002	F_{40}	1670	1770	1640
PF6320	F_{60}	3480	3580	4740

[a] These molecular weights were provided by the manufacturer.[1]

which was stirred for 10 min under an inert nitrogen atmosphere. The solution was heated to 50°C and *p*-nitrobenzoyl chloride (22.48 g, 0.121 mol) dissolved in toluene (150 mL) was added drop-wise over 30 min. The solution was heated to reflux and stirred overnight. The reaction mixture was cooled to room temperature, filtered, washed with 5% $NaHCO_3$ (250 mL × 2) and deionized water (250 mL × 2), dried with $MgSO_4$, and the solvent was removed using a rotary evaporator. The resultant viscous light amber liquid was vacuum dried to yield 64.94 g (90%) of a clear amber viscous liquid.

NO_2-Terminated F_{18}

^{1}H NMR (300 MHz, $CDCl_3$) δ 0.8–0.9 (*m*, 16 H, methyl), 1.0–1.1 (*m*, 6 H, AEFO methyl groups in end repeat unit), 3.1–3.6 (*m*, 36 H, methylene in AEFO backbone and in side chain), 3.7–3.9 (*m*, 11 H, methylene adjacent to fluorinated carbon), 4.3 (*m*, 4 H, methylene in AEFO backbone in end repeat unit), 8.2 (d, 4 H, Ar), 8.3 (d, 4H, Ar); ^{13}C NMR (75.5 MHz, $CDCl_3$) δ 17.4, 17.5, 21.6, 22.3, 26.6, 36.2, 36.9, 40.8, 41.4, 41.5, 68.1, 69.1 (q), 71.4, 71.8, 73.5, 73.8, 75.3, 75.4, 122.4, 123.8, 126.1, 130.9, 135.8, 150.8, 164.7.

NO_2-Terminated F_{30}

^{1}H NMR (300 MHz, $CDCl_3$) δ 0.8–0.9 (*m*, 14 H, methyl), 1.0–1.1 (*m*, 6 H, methyl groups in end repeat unit), 3.1–3.6 (*m*, 32 H, methylene in AEFO backbone and in side chain), 3.8–3.9 (*m*, 10 H, methylene adjacent to fluorinated carbon), 4.3 (*m*, 4 H, methylene in AEFO backbone in end repeat unit), 8.2 (d, 4 H, Ar), 8.3 (d, 4H, Ar); ^{13}C NMR (75.5 MHz, $CDCl_3$) δ 17.2, 17.3, 21.6, 22.2, 26.6, 36.1, 36.8, 40.8, 41.4, 41.5, 68.1 (q), 68.3, 71.4, 71.7, 71.8, 73.4, 73.9, 75.5, 78.0, 111.8, 118.9 (*t*), 123.8, 124.3, 130.7, 131.95, 135.7, 150.8, 164.7.

NO_2-Terminated F_{30B}

^{1}H NMR (300 MHz, $CDCl_3$) δ 0.9 (*m*, 14 H, methyl), 1.1 (s, 4 H, methyl groups in end repeat unit), 3.1–3.5 (*m*, 35 H, methylene in AEFO backbone and in side chain), 3.7 (*m*, 120 H, methylene in polyethylene glycol (PEG) repeat unit), 3.8–3.9 (*m*, 14 H, methylene adjacent to fluorinated carbon), 4.3 (*m*, 3 H, methylene in AEFO backbone in end repeat unit), 8.2 (*d*, 4 H, Ar), 8.3 (*d*, 4H, Ar); ^{13}C NMR (75.5 MHz, $CDCl_3$) δ 17.3, 17.5, 26.5, 40.6, 40.8, 41.4, 41.5, 65.1, 68.1, 68.3 (*t*), 70.5, 70.8, 71.1, 71.4, 71.8, 73.4, 73.8, 75.5, 120.8 (*t*), 123.8, 130.8, 131.1, 135.7, 150.8, 164.6, 164.9.

NO_2-Terminated F_{40}

^{1}H NMR (300 MHz, $CDCl_3$) δ 0.8–1.0 (*m*, 18 H, methyl), 2.3 (*m*, 8 H, methylene adjacent to fluorinated carbon chain), 3.1–3.4 (*m*, 26 H, methylene in AEFO backbone and in sidechain), 3.6–3.7 (*m*, 7 H, methylene one carbon removed from fluorinated carbon chain), 4.2–4.3 (*m*, 4 H, methylene in AEFO backbone in end repeat unit), 8.2 (*d*, 4 H, Ar), 8.3 (*d*, 4H, Ar); ^{13}C NMR (75.5 MHz, $CDCl_3$) δ 17.5, 21.6, 22.2, 26.6, 31.5 (*t*), 36.1, 36.9, 40.6, 41.1, 41.4, 63.3, 68.4, 73.9 (*t*), 118.1, 123.7, 124.4, 130.8, 135.9, 150.8, 164.7.

NO_2-Terminated F_{60}

^{1}H NMR (300 MHz, $CDCl_3$) δ 0.8–0.9 (*m*, 53 H, methyl), 1.1 (*m*, 6 H, methyl groups in end repeat unit), 3.2–3.6 (*m*, 122 H, methylene in AEFO backbone and in side chain), 3.7–3.8 (*m*, 41 H, methylene adjacent to fluorinated carbon), 4.3 (*m*, 4 H, methylene in AEFO backbone in end repeat unit), 8.2 (*d*, 4 H, Ar), 8.3 (*d*, 4H, Ar); ^{13}C NMR (75.5 MHz, $CDCl_3$) δ 17.3, 17.5, 26.6, 40.8, 41.4, 41.6, 68.2, 69.1 (q), 71.4, 71.8, 73.3, 73.4, 73.9, 75.4, 122.5, 123.8, 124.4, 130.8, 135.8, 150.8, 164.7.

Synthesis of Amine-Terminated AEFOs

The nitro end-groups were reduced in a hydrogen atmosphere using an ethanol solution of 5% Pd/C as a catalyst and mechanical agitation. As an example, a hydrogenation reactor bottle was charged with the nitro-terminated AEFO (NO_2-terminated F_{40}, 14.6 g), 5% Pd/C catalyst (0.6 g), and ethanol (200 mL, 200 proof). The bottle was connected to the hydrogenation reactor using a rubber stopper with an H_2 gas inlet. The bottle was evacuated and mechanical agitation was initiated. H_2 was slowly added to the reaction bottle up to a pressure of 25 psi. Additional H_2 was added to the reaction bottle as it was consumed. Initially, the pressure dropped rapidly indicating that the reduction reaction was proceeding. After approximately 1 h, the pressure reduction slowed and after 4 h, the pressure was brought to 30 psi by the addition of H_2. The mechanical agitation reactor was run overnight. The reaction mixture was filtered through a Buchner funnel with filter paper and a layer of celite followed by solvent removal via rotary evacuation. The recovered product, an amber oil, was held under vacuum for an additional 4 h to remove any remaining EtOH. The final product mass was 13.8 g indicating a reaction yield approaching 100%.

NH_2-Terminated F_{18}

^{1}H NMR (300 MHz, $CDCl_3$) δ 0.8–0.9 (*m*, 15 H, methyl), 1.03–1.04 (*m*, 4 H, methyl groups in end repeat unit), 3.1–3.6 (*m*, 33 H, methylene in AEFO backbone and in side chain), 3.7–3.9 (*m*, 11 H, methylene adjacent to fluorinated carbon), 4.0–4.2 (*m*, 7 H, methylene in AEFO backbone in end repeat unit), 6.6 (*d*, 4 H, Ar), 7.8 (*d*, 4H, Ar); ^{13}C NMR (75.5 MHz, $CDCl_3$) δ 17.4, 17.5, 22.3, 26.6, 36.2, 36.9, 40.8, 41.4, 41.6, 66.6, 69.2 (q), 69.9, 71.4, 71.9, 73.6, 73.9, 75.4, 114.0, 119.8, 122.4, 126.1, 131.9, 132.5, 151.2, 166.6.

NH_2-Terminated F_{30}

^{1}H NMR (300 MHz, $CDCl_3$) δ 0.8–1.0 (*m*, 21 H, methyl), 3.1–3.5 (*m*, 33 H, methylene in AEFO backbone and in side chain), 3.7–3.9 (*m*, 12 H, methylene adjacent to fluorinated carbon), 4.2 (*m*, 4 H, methylene in AEFO backbone in end repeat unit), 6.6 (*d*, 4 H, Ar), 7.8 (*d*, 4H, Ar); ^{13}C NMR (75.5 MHz, $CDCl_3$) δ 17.2, 17.3, 22.2, 26.6, 36.1, 36.9, 40.9, 41.4, 41.5, 66.6, 68.4 (*t*), 71.4, 71.7, 73.5, 73.9, 75.6, 114.0, 119.9, 120.9, 131.7, 151.1, 166.5.

NH_2-Terminated F_{30B}

^{1}H NMR (300 MHz, $CDCl_3$) δ 0.9 (*m*, 14 H, methyl), 1.0 (*m*, 5 H, methyl groups in end repeat unit), 3.1–3.5 (*m*, 37 H, methylene in AEFO backbone and in side chain), 3.6 (*m*, 125 H, methylene in PEG repeat unit), 3.7–3.9 (*m*, 15 H, methylene adjacent to fluorinated carbon), 4.1–4.3 (*m*, 4 H, methylene in AEFO backbone in end repeat unit), 6.6 (*d*, 4 H, Ar), 7.8 (*d*, 4H, Ar); ^{13}C NMR (75.5 MHz, $CDCl_3$) δ 17.3, 17.5, 26.6, 40.7, 40.9, 41.4, 41.5, 63.8, 66.5, 68.2 (*t*), 70.6, 70.8, 71.1, 71.4, 71.8, 73.4, 73.8, 75.4, 114.0, 131.7, 132.0, 151.5, 166.6.

NH_2-Terminated F_{40}

^{1}H NMR (300 MHz, $CDCl_3$) δ 0.8–1.0 (*m*, 18 H, methyl groups), 2.3 (*m*, 8 H, methylene adjacent to fluorinated carbon

chain), 3.1–3.4 (*m*, 26 H, methylene in AEFO backbone and in side chain), 3.6–3.7 (*m*, 7 H, methylene one carbon removed from fluorinated carbon chain), 4.1–4.2 (*m*, 4 H, methylene in AEFO backbone in end repeat unit), 6.6 (*d*, 4 H, Ar), 7.8 (*d*, 4H, Ar); ^{13}C NMR (75.5 MHz, $CDCl_3$) δ 17.5, 18.6, 22.3, 26.6, 31.5 (*t*), 36.9, 40.7, 41.4, 58.6, 63.3, 67.0, 70.0, 74.0 (*t*), 114.0, 118.1, 120.1, 131.8, 132.4, 151.1, 166.7.

NH_2-Terminated F_{60}

^{1}H NMR (300 MHz, $CDCl_3$) δ 0.9 (*m*, 65 H, methyl), 1.0 (s, 6 H, methyl groups in end repeat unit), 3.1–3.5 (*m*, 147 H, methylene in AEFO backbone and in sidechain), 3.7–3.8 (*m*, 52 H, methylene adjacent to fluorinated carbon), 4.2 (*m*, 4 H, methylene in AEFO backbone in end repeat unit), 6.6 (*d*, 4 H, Ar), 7.8 (*d*, 4H, Ar); ^{13}C NMR (75.5 MHz, $CDCl_3$) δ 17.3, 17.5, 26.5, 40.8, 41.4, 41.6, 66.7, 69.1 (q), 71.5, 71.8, 73.3, 73.5, 73.8, 75.4, 114.0, 120.0, 122.5, 126.3, 130.0, 131.8, 151.1, 166.7.

Synthesis of Copoly(imide alkyl ether)s

Homopolyimides prepared by the condensation reaction of stoichiometric equivalents of s-BPDA and 4-4′-ODA were observed to be far too viscous to fabricate quality film samples as will be described below. Therefore, a ratio of diamine: dianhydride of 0.85 : 1 was used for the synthesis of all the polymer systems described in this work including a control synthesized without any amine-terminated AEFO. To prepare the homopolyimides, a reaction vessel was flushed with nitrogen for 10 min before the addition of reactants. Reactions were carried out under nitrogen at 20 wt % solids in dimethylacetamide (DMAc). The diamine (typically 7–10 mmol) was dissolved in DMAc (typically 15 mL), to which the dianhydride (typically 7–10 mmol) was added, followed by additional DMAc (for a total of 40 mL), and the reaction mixture was mechanically stirred overnight. Inherent viscosities (η_{inh}) were determined at 25°C using the poly(amide acid) solutions and an Ubbelohde viscometer at solution concentrations of 0.5 g dL^{-1}. Films were subsequently cast on plate glass using a doctor blade and placed in a forced-air drying chamber until tack-free. Films were then thermally imidized under nitrogen using a cure cycle with stages at 150, 175, 200, and 250°C, with at least a 40 min hold at each temperature. Complete imidization under these conditions was confirmed by attenuated total reflection Fourier transformed infrared spectroscopy (ATR-FTIR, data not shown). The films were removed from the glass and used to perform the various characterizations and tests described herein. Synthesis of the copolymer samples was performed similarly with the amine-terminated AEFO oligomers added to the reaction flask at the same time as the diamine. This diamine mixture was stirred mechanically for approximately 10 min before the addition of the dianhydride. For these reactions, the homopolyimide and copolymers were obtained in nearly quantitative yield.

As five different AEFO oligomers were used at loading levels from 0.01 wt % to 5 wt % to generate copolymer samples, a nomenclature system will be used here to facilitate discussion. The copolymers will be referred to as PIAE for copoly(imide alkyl ether) with the relevant AEFO oligomer appended according to the previously described designation by the number of fluorine atoms per oligomer (Table I). Designation of the AEFO loading level will be described by a number in parentheses. Thus, a copoly(imide alkyl ether) synthesized using F_{18} (PF636) at a loading level of 0.05 wt % would be designated as $PIAEF_{18}(0.05)$. All of the synthesized copolymer samples are shown in Table II by their designations.

RESULTS AND DISCUSSION

End-Group Functionalization of AEFO Oligomers

AEFO oligomers were end-group functionalized with primary amines to enable reaction directly into the backbone of a polyimide synthesized from dianhydride and diamine aromatic monomers. This was achieved by reacting the hydroxyl end-groups with 4-nitrobenzoyl chloride generating nitro end-groups (Scheme 2). Reduction to the amine-terminated AEFO was achieved using H_2 with 5% Pd/C as a catalyst.

^{1}H NMR was used to determine the molecular weight of the functionalized oligomers after both the nitration and amine formation steps. As the AEFO oligomer is aliphatic, the aromatic protons arising from the presence of the 4-nitro benzoate functionality were readily identified. With the nitro functionality, these protons were located at 8.2 and 8.3 PPM and were assigned to the protons meta and ortho to the nitro functionality, respectively. Upon reduction to the amine, these protons undergo a readily noticeable shift to 7.8 and 6.6 PPM, respectively. For both the nitro- and amine-terminated oligomers, the aromatic protons assigned to the ortho position, relative to the C—N bond, were assigned a proton value of 4. Using this weighting, the AEFO oligomer methyl group protons and methylene protons were next identified and their integrations weighted according to the aromatic signal values. Finally, the signal arising from the methylene protons adjacent to the fluorinated carbon chain were identified and their integration values determined. By using these three proton assignments (methyl groups, methylene groups, and the methylene protons adjacent to the fluorinated carbon chain), the number of repeat units in the oligomers could be calculated. The average of these three values was taken to be the molecular weight of the end-group functionalized AEFO oligomers. These values along with the molecular weights of the as-received hydroxyl-terminated oligomers, as provided by the manufacturer, are shown in Table I. In general, the AEFO oligomer molecular weight increased relative to the molecular weight provided by the manufacturer through the course of the end-group functionalization reactions. Although not confirmed, one likely explanation was that cyclic structures, known to be a common contaminant in oxetane-derived oligomers,[11,16] were removed during the product purification processes. The one exception to this was the F_{30B} oligomer for which the molecular weight decreased considerably. As this oligomer has a tri-block structure with two oxetane-derived blocks connected by a PEG central unit, it is plausible that cyclic contamination was not as prevalent in this material. Gel permeation chromatography (GPC) would offer insight into the molecular weight distribution of these oligomers but was not available during the course of this study.[26]

Copolyimide Synthesis

Condensation polymerization of the aromatic dianhydride (s-BPDA) with the aromatic diamine (4,4′-ODA), and the

Table II. Copoly(imide alkyl ether) Inherent Viscosity Values, From the Amide Acid Intermediate, and Polymer Film Mechanical Properties

Copolymer	η_{inh} (dL g^{-1})	Tensile modulus (MPa)	Break stress (MPa)	% Elongation at break
PI, no offset	2.8	–[a]	–[a]	–[a]
PI, with offset	1.4	3590 ± 110	175 ± 16	10 ± 3
PIAEF$_{18}$(0.01)	0.9	3330 ± 40	130 ± 6	11 ± 3
PIAEF$_{18}$(0.05)	1.2	3280 ± 30	129 ± 12	9 ± 3
PIAEF$_{18}$(0.1)	1.3	3270 ± 190	128 ± 8	9 ± 3
PIAEF$_{18}$(0.5)	1.1	3150 ±	137 ±	10 ±
PIAEF$_{18}$(1)	1.1	3230 ± 50	132 ± 3	9 ± 2
PIAEF$_{18}$(5)	1.5	3010 ± 70	119 ± 3	8 ± 1
PIAEF$_{30}$(0.01)	1.0	3450 ± 80	139 ± 3	10 ± 1
PIAEF$_{30}$(0.05)	0.9	3330 ± 50	138 ± 5	11 ± 3
PIAEF$_{30}$(0.1)	0.8	3230 ± 20	130 ± 3	8 ± 1
PIAEF$_{30}$(0.5)	0.8	3210 ± 60	124 ± 6	10 ± 2
PIAEF$_{30}$(1)	0.8	3190 ± 110	129 ± 6	9 ± 3
PIAEF$_{30}$(5)	0.7	3140 ± 80	126 ± 2	13 ± 1
PIAEF$_{30B}$(0.01)	0.8	3110 ± 40	137 ± 4	11 ± 3
PIAEF$_{30B}$(0.05)	0.8	2950 ± 70	134 ± 4	15 ± 5
PIAEF$_{30B}$(0.1)	0.9	3040 ± 50	133 ± 4	12 ± 4
PIAEF$_{30B}$(0.5)	0.9	2940 ± 50	130 ± 5	12 ± 5
PIAEF$_{30B}$(1)	1.0	3010 ± 60	134 ± 3	11 ± 3
PIAEF$_{30B}$(5)	0.9	2690 ± 40	119 ± 2	15 ± 3
PIAEF$_{40}$(0.01)	1.2	3390 ± 150	131 ± 17	10 ± 3
PIAEF$_{40}$(0.1)	1.2	3470 ± 80	141 ± 8	8 ± 2
PIAEF$_{40}$(0.5)	1.1	3460 ± 50	133 ± 5	11 ± 1
PIAEF$_{40}$(1)	1.2	3510 ± 70	138 ± 6	9 ± 2
PIAEF$_{40}$(5)	1.2	3250 ± 70	126 ± 3	10 ± 3
PIAEF$_{60}$(0.01)	1.4	3560 ± 40	142 ± 3	8 ± 2
PIAEF$_{60}$(0.05)	1.5	3570 ± 80	139 ± 11	8 ± 2
PIAEF$_{60}$(0.1)	1.2	3570 ± 80	142 ± 3	9 ± 2
PIAEF$_{60}$(0.2)	1.2	3500 ± 60	139 ± 4	12 ± 2
PIAEF$_{60}$(0.4)	1.3	3450 ± 60	138 ± 6	8 ± 2
PIAEF$_{60}$(0.5)	1.1	3350 ± 160	142 ± 4	6 ± 2
PIAEF$_{60}$(0.8)	1.0	3460 ± 70	138 ± 3	11 ± 1
PIAEF$_{60}$(1)	1.6	3440 ± 70	141 ± 3	9 ± 1
PIAEF$_{60}$(2)	1.2	3380 ± 50	138 ± 3	9 ± 1
PIAEF$_{60}$(5)	1.3	3140 ± 60	126 ± 2	10 ± 2

[a] The viscosity of this poly(amide acid) solution was too high to cast films preventing determination of mechanical properties.

amine-terminated AEFO yielded the copoly(imide alkyl ether)s described in this work (Scheme 3). This synthetic approach would yield random copolymers. After purification by refluxing the s-BPDA in an acetic acid : acetic anhydride solution, homopolyimides were synthesized, i.e., no AEFO oligomer, to further evaluate monomer purity. These monomers were reacted in DMAc at 20 wt % solids to generate the polyamide acid intermediate which was used to determine inherent viscosity (η_{inh}) values. Using a stoichiometrically equivalent amount of each monomer resulted in a highly viscous polyamide acid solution (Table II). Although this confirmed the purity of the monomers, the viscosity was too high to readily prepare polymer film samples via solution casting without further dilution of the poly(amide acid) solution. Therefore, different stoichiometric offset ratios were evaluated with the dianhydride in excess, to identify a homopolyimide composition that would yield reasonable inherent viscosity values. Ultimately, a diamine : dianhydride ratio of 0.85 : 1 was chosen as this stoichiometric offset yielded a polyamide acid of reasonably high molecular weight without the viscosity being so high as to hinder film casting. This stoichiometric offset was used for all of the copolymers synthesized in this work.

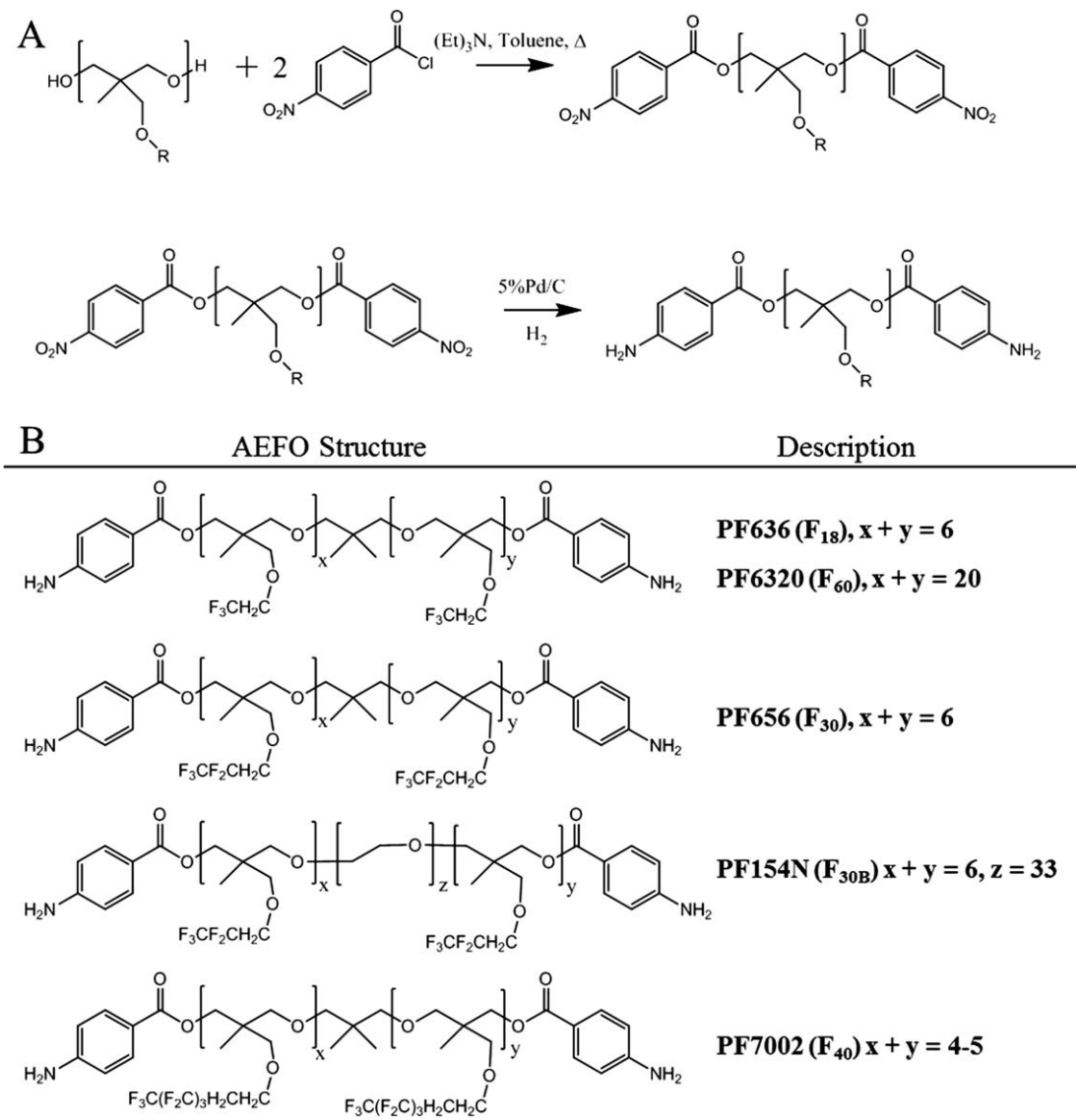

Scheme 2. (A) AEFO end-group functionalization and (B) AEFO oligomers used in this work.

The inherent viscosities ranged from 0.7 to 1.6 dL/g, indicating that all of the polymers synthesized were of relatively high molecular weight. Similarly, for each AEFO oligomer series, the inherent viscosity did not differ dramatically at the two AEFO loading extremes, 0.01 wt % and 5 wt %. In general, the copoly(imide alkyl ether)s synthesized with fluorinated ethylene

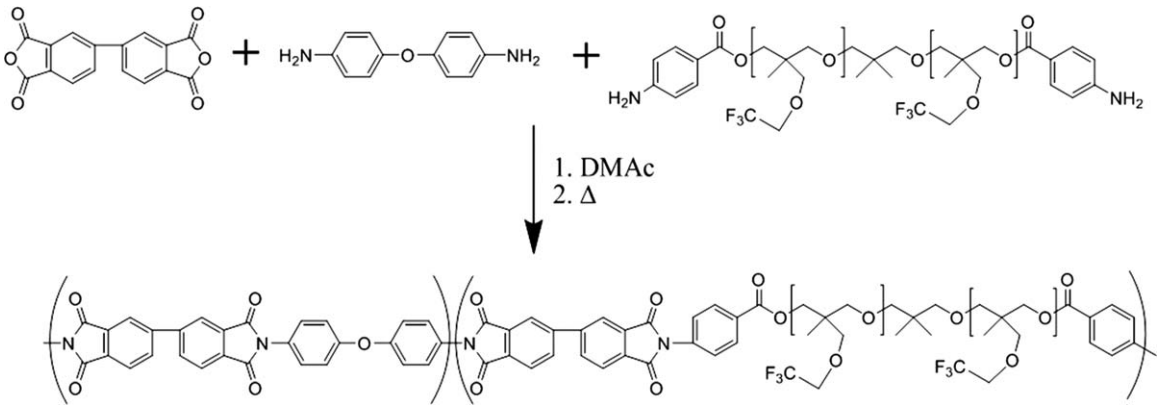

Scheme 3. Copolymer synthesis with the synthesis of $PIAEF_{18}$ shown as an example.

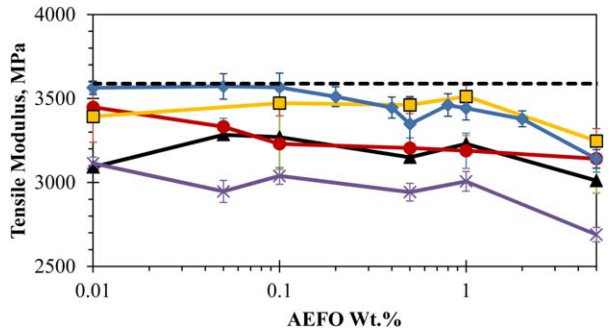

Figure 1. Tensile modulus measured on copolymer films synthesized with F_{18} (black triangles), F_{30} (red circles), F_{30B} (purple asterisks), F_{40} (orange squares), and F_{60} (blue diamonds) AEFO oligomers. The modulus measured for the homopolyimide is also included (dashed line) for comparison. [Color figure can be viewed in the online issue, which is available at wileyonlinelibrary.com.]

pendant groups were determined to have lower inherent viscosity values than either the fluorinated methyl or butyl containing polymers. The PEG-containing AEFO, F_{30B}, may act as an amphiphilic species in solution preferentially segregating to the polymer/solution interface resulting in polymers with smaller hydrodynamic radii relative to the other copoly(imide alkyl ether)s. The fluorinated butyl AEFO, F_{40}, may conversely form micelle-like aggregates within the copolymer matrix enabling the surrounding aromatic amide acid species to become more swollen by solvent and increasing the hydrodynamic radius. In both of these instances, the presence of PEG groups at the copolymer/solvent interface and formation of micelle-like fluorinated species within the copolymer matrix should also influence the surface properties as will be discussed below.

The solution cast, thermally imidized, copolymer film transparency was similar to the homopolymer film for all of the AEFO oligomers and at all AEFO loading levels except at 5 wt % AEFO. For every oligomer, films generated from copolymers with 5 wt % AEFO were markedly more opaque. This could arise from phase segregation in the copolymer bulk as has been seen for similar copolyimide systems.[27] All of the films generated in this work were creasable as determined by folding a small portion of the film and verifying that the film did not crack at the seam. Although the glass transition temperature, T_g, of this homopolyimide has been studied extensively using a variety of techniques,[28] differential scanning calorimetry (DSC) experiments performed with these materials did not provide endothermic peaks of significant magnitude. This could be due to the relatively small segment motion that these materials undergo during this transition.

Tensile Properties of Copolymer Films

Samples were cut from the copolymer films to determine the impact AEFO oligomers have on the mechanical properties relative to the homopolyimide. These specimens were tested under tension to failure and tensile modulus, break stress, and percent elongation at break were determined (Table II). Although there was some variation among the tensile modulus values, in general the measured tensile properties were within the range expected for typical imide materials.[29] An increase in AEFO content resulted in only a slight decrease in modulus (Figure 1). The lowest tensile modulus values were measured from films generated from the F_{30B}-containing copolymers, which may be attributed to the PEG functionalities in the AEFO oligomer backbone enabling slightly better phase mixing relative to the other AEFO oligomers. In general, addition of the AEFO oligomers did not change the percent elongation values or break stress values considerably.

Surface Characterization of Copolymer Films

CAG was utilized to provide insight into the structure–property relationships for the AEFO oligomers studied in this work.

Table III. Water Contact Angle Values from Measurements on the Air and Glass Sides of Copoly(imide alkyl ether) Films

	Water contact angle (°)	
Copolymer	Air side	Glass side
PI, with offset	80 ± 2	70 ± 2
PIAEF$_{18}$(0.01)	78 ± 3	73 ± 3
PIAEF$_{18}$(0.05)	86 ± 2	78 ± 2
PIAEF$_{18}$(0.1)	83 ± 1	74 ± 1
PIAEF$_{18}$(0.5)	86 ± 2	80 ± 2
PIAEF$_{18}$(1)	108 ± 4	88 ± 2
PIAEF$_{18}$(5)	103 ± 5	69 ± 3
PIAEF$_{30}$(0.01)	86 ± 1	64 ± 5
PIAEF$_{30}$(0.05)	91 ± 1	67 ± 3
PIAEF$_{30}$(0.1)	89 ± 4	76 ± 2
PIAEF$_{30}$(0.5)	90 ± 2	85 ± 3
PIAEF$_{30}$(1)	94 ± 4	86 ± 8
PIAEF$_{30}$(5)	91 ± 3	87 ± 2
PIAEF$_{30B}$(0.01)	87 ± 1	75 ± 3
PIAEF$_{30B}$(0.05)	88 ± 1	73 ± 2
PIAEF$_{30B}$(0.1)	79 ± 1	77 ± 2
PIAEF$_{30B}$(0.5)	92 ± 1	80 ± 1
PIAEF$_{30B}$(1)	95 ± 1	73 ± 2
PIAEF$_{30B}$(5)	92 ± 1	86 ± 2
PIAEF$_{40}$(0.01)	96 ± 2	62 ± 6
PIAEF$_{40}$(0.1)	98 ± 1	65 ± 2
PIAEF$_{40}$(0.5)	98 ± 1	82 ± 2
PIAEF$_{40}$(1)	98 ± 1	82 ± 2
PIAEF$_{40}$(5)	98 ± 1	83 ± 2
PIAEF$_{60}$(0.01)	93 ± 1	68 ± 4
PIAEF$_{60}$(0.05)	95 ± 1	63 ± 1
PIAEF$_{60}$(0.1)	95 ± 1	68 ± 1
PIAEF$_{60}$(0.2)	95 ± 1	57 ± 1
PIAEF$_{60}$(0.4)	94 ± 1	65 ± 2
PIAEF$_{60}$(0.5)	94 ± 2	62 ± 1
PIAEF$_{60}$(0.8)	94 ± 1	59 ± 1
PIAEF$_{60}$(1)	98 ± 1	78 ± 4
PIAEF$_{60}$(2)	94 ± 1	72 ± 2
PIAEF$_{60}$(5)	95 ± 1	62 ± 1

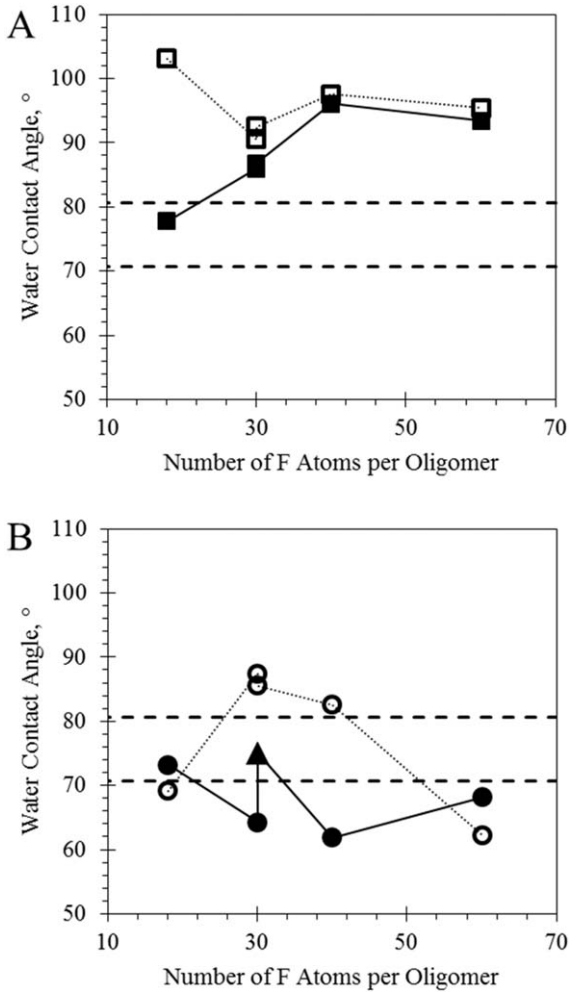

Figure 2. Water contact angle values measured on the air side (A, squares) and glass side (B, circles) of solution cast polymer films. The minimal and maximal loading levels, 0.01 wt % (filled symbols, solid line) and 5 wt % (open symbols, dashed line), respectively, indicated that the surface properties were both AEFO and loading level dependent. As both F_{30} and F_{30B} containing copolymers have 30 fluorine atoms per repeat unit, a triangle symbol was used to indicate the F_{30B} value when their values differed by greater than 2°. The contact angle values determined for the homopolyimide are included as dashed lines for the air side (80.6°) and glass side (70.7°).

Water contact angle measurements were collected on both the air and glass sides of the copolymer films to characterize the surface migration behavior of the fluorinated AEFO moieties. Water contact angle values were higher for the copolymer film samples relative to the homopolyimide (Table III). The water contact angle value on the air side of the copolymer films was greater for every AEFO studied at 5 wt % loading compared with the homopolyimide. Interestingly, the largest water contact angle value was measured on the copolymer film fabricated from the AEFO with the smallest fluorinated side chain, F_{18}. This value (108° at 1 wt %) is similar to values obtained on perfluorinated surfaces such as polytetrafluoroethylene, which has water contact angle values ranging from 105° to 120°. The higher water contact angle value exhibited by this AEFO, relative to the other copolymer films may arise from reduced steric hindrance of this oxetane to populate the surface compared with the other AEFO that have larger fluorinated side chains or/and higher molecular weights. At 0.01 wt % AEFO loading, the F_{40} oligomer exhibited the largest water contact angle value measured. With the largest perfluorinated side chain, the F_{40} oligomer would be anticipated to migrate to and orient at the surface more efficiently than the other oligomers. Water contact angle values measured on the glass side of the copolymer films were generally greater than that measured on the homopolyimide but lower than the values measured on the air side.

There was significant variation in water contact angle value change as a function of increased loading for the different AEFO oligomers. For example, the smallest AEFO, F_{18}, exhibited an increase in water contact angle of 25° from 0.01 wt % to 5 wt %, while the largest AEFO, F_{60}, exhibited an increase of only 2° over the same loading level range [Figure 2(A)]. Similarly, the AEFO with the largest fluorinated side chain, F_{40}, also only exhibited a water contact angle value increase of 2°. Micelle formation in the bulk may explain this observation. Micelle formation may be a more favorable pathway for limiting perfluoro group/matrix interaction relative to surface migration that may be sterically hindered as previously mentioned, which is in agreement to what was observed for similar perfluorinated oligomer containing systems.[2] Addition of AEFO oligomers with either of the fluorinated ethylene side chains produced modest increases in water contact angle values over this loading level range.

Water contact angle values measured on the glass side of the copolymer films are also plotted in Figure 2(B). Interestingly, water contact angle values measured on the glass side of the PEG-containing AEFO, F_{30B}, copolymer film were greatest at 0.01 wt % relative to the other AEFO oligomer-containing films. The apparent preference of this oligomer to migrate to interfacial regions suggests that this particular AEFO has more of an amphiphilic nature than the other oxetane oligomers investigated here, i.e., the PEG groups may have been drawn to the interface as a result of hydroxyl groups present on the glass surface of the substrate. Water contact angle values measured on the copolymer films' glass side synthesized from AEFO with

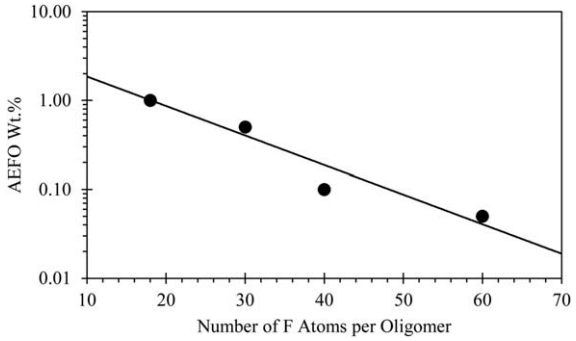

Figure 3. AEFO surface loading limit levels for each AEFO oligomer determined as the loading level at which the determined water contact angle was no less than 1° lower than the value measured at 5 wt %. The solid line is an exponential function fit to the data.

Table IV. XPS Results for $PIAEF_{60}$ Film Samples

	Atomic percentage, air side (glass side)				
Copolymer	*F*	C	O	N	Surface excess (z^*), mol/m^2 ($\times 10^{-6}$)
PI, Offset	5.2 (1.6)	74.1 (73.5)	15.1 (16.6)	4.3 (4.3)	–
$PIAEF_{60}(0.1)$	14.3 (5.2)	70.0 (72.9)	15.7 (16.5)	0 (3.9)	1.04
$PIAEF_{60}(0.2)$	14.4	66.3	16.2	2.8	1.04
$PIAEF_{60}(0.4)$	20.0	63.7	16.3	0	1.68
$PIAEF_{60}(0.5)$	15.7 (8.9)	64.4 (66.1)	16.5 (19.5)	3.1 (2.5)	1.18
$PIAEF_{60}(0.8)$	16.8	65.1	15.8	2.4	1.30
$PIAEF_{60}(1)$	18.5 (8.1)	61.6 (71.8)	16.7 (15.3)	1.7 (3.5)	1.49
$PIAEF_{60}(2)$	17.2	64.2	16.2	2.3	1.31
$PIAEF_{60}(5)$	18.0 (4.4)	65.5 (71.2)	16.5 (19.1)	0 (3.4)	1.32

fluorinated methyl groups, F_{18} and F_{60}, were significantly smaller than values measured on the other copolymer films at 5 wt % AEFO. In fact, the copolymer films synthesized from fluorinated methyl group AEFO exhibited water contact angle values at or below the value measured on the glass side of the homopolyimide film.

According to Table III and Figure 2, there appeared to be a loading limit beyond which an increase in the AEFO loading did not increase the water contact angle values measured on the air side of the copolymer films. Based on the collected data, this loading limit was determined for each AEFO oligomer and compared with the number of fluorine atoms per oligomer (Figure 3). As may be expected, as the number of fluorine atoms per oligomer increased, the required AEFO loading to maximally populate the surface decreased. Similarly, the AEFO oligomers with both the lowest and greatest number of fluorine atoms, F_{18} and F_{60}, which both have the same fluorinated CF_3 moiety, exhibited very different loading limit levels, 1 wt % and 0.05 wt %. This may be attributed to a better separation of the F_{60} oligomers from the surrounding imide matrix relative to the smaller F_{18} oligomers. The data in Figure 3 can be fitted reasonably well with a simple exponential function. Using this function, the loading limit level for different fluorine-containing AEFOs in copolyimide systems can be predicted and focused studies around that loading level can be conducted.

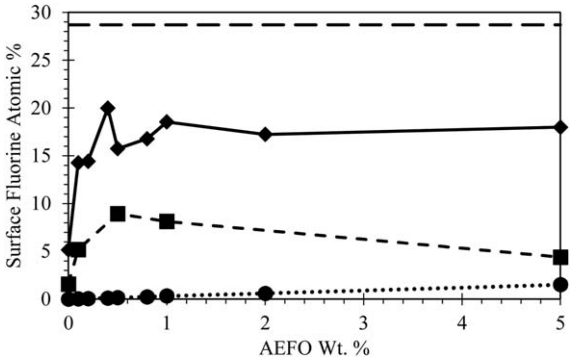

Figure 4. Surface fluorine atomic percentages were determined by XPS on $PIAEF_{60}$ copolymer film air (diamonds, solid line) and glass (squares, dashed line) sides. The bulk fluorine atomic percentage (circles, dotted line) was calculated based upon reaction masses. The fluorine atomic percentage for a pure F_{60} oligomer (28.7% based upon the chemical structure, long dashed line) is also included for comparison.

With the apparently low loading limit level determined for the F_{60}-containing copolyimide, XPS measurements were conducted on both the air and glass sides. The slightly deeper sampling depth of XPS (3–10 nm)[30] relative to CAG was thought to provide further insight into the migration behavior of this AEFO. The surface atomic concentrations determined from low resolution spectra are shown in Table IV. As the films were cast on glass, the glass sides of the films typically have silicon-based contaminants. Silicon was typically at concentrations lower than 1% and is not shown in Table IV. Similarly, the background fluorine level, of particular interest to this analysis, was approximately 5% based on the measured concentration on the homopolyimide surface. As can be seen in Table IV, increasing the AEFO content increased the fluorine and oxygen concentration while reducing the carbon content. Fluorine concentrations were significantly greater than what would be predicted based on the monomer masses. This was further verification of the surface migration of the fluorinated AEFO oligomers as their fluorine and oxygen content is greater than that for the imide portions which have no fluorinated substituents.

Comparison of the fluorine concentration and AEFO content enabled determination of the loading limit level (Figure 4), similar to the determination from advancing water contact angle values. Based on the apparent variability of fluorine concentrations of 3–5%, the loading limit level determined according to XPS was 0.5 wt % which is an order of magnitude higher than that determined according to the CAG results (0.05 wt %). For comparison, two reference lines are included in Figure 4. The large dashed line, at a fluorine atomic concentration of 28.7%, corresponds to what the calculated fluorine atomic concentration would be for a surface comprised of only F_{60} AEFO oligomers. The dotted line with circular data points is the calculated fluorine concentration for the bulk copolymer based on reaction masses. As can be seen, the fluorine atomic

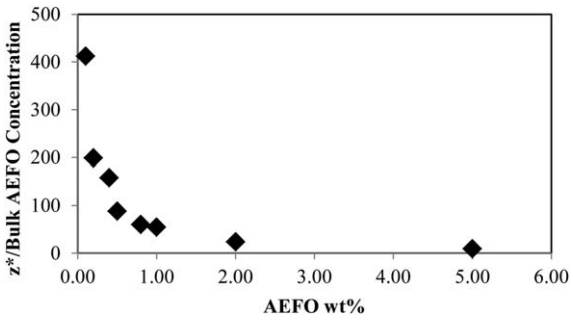

Figure 5. Ratio of z^* and the concentration of AEFO in the bulk for the same interfacial area calculated at different AEFO loading levels determined from XPS F atomic % values.

concentration is significantly higher than that calculated from the monomer masses, albeit lower than that calculated for a pure AEFO layer. This is in agreement with the CAG results that indicated steric hindrance or/and bulk micelle formation may prevent AEFO oligomers from completely covering the surface, especially for the large oligomers such as F_{60}.

Migration of the AEFO oligomers to the surface was verified by CAG and XPS. According to the XPS results, the PIAEF$_{60}$ loading limit was determined to be approximately 0.5 wt % with a fluorine atomic concentration of 15.7%. At this AEFO loading level the fluorine atomic concentration for the bulk should only be 0.2%. Alternatively, if the surface was composed only of the AEFO moiety, the fluorine atomic concentration should be approximately 28.7%. Therefore the surface must be populated by a combination of both AEFO and imide oligomers.

Surface fluorine atomic concentration does not increase considerably at loading levels above 0.5 wt % suggesting that any additional AEFO results in bulk aggregation which may be similar to micelle formation in surfactant systems above the critical micelle concentration. By using the relative atomic concentration of fluorine at the surface for different AEFO loading levels, AEFO surface concentrations can be calculated and, when compared with the reaction stoichiometry, can be used to experimentally determine a surface excess concentration, z^*:

$$z^* = \int_0^\infty \phi(x) - \phi_{\text{bulk}}\, dx \qquad (1)$$

where $\phi(x)$ is the concentration of AEFO as a function of depth, x, and ϕ_{bulk} is the bulk AEFO concentration.

As the probe depth of XPS is approximately 3–10 nm,[30] we can define our surface volume as the space occupied by the polymer film to this depth (10 nm) with the remaining mass being considered bulk material. (For this analysis, we will consider the separation between the bulk and surface concentrations to be distinct, i.e., a very abrupt change in the concentration of the fluorinated species upon traversing through the film thickness beyond the 10-nm depth. More realistically, it is likely that there is a surface concentration layer followed by a monotonic decrease in concentration approaching bulk values.[31]) Taking a 1 cm^2 sample of the polymer film and using the average film thickness, 4.55×10^{-3} cm, the surface volume would be 1×10^{-6} cm^3 while the bulk volume would be the remainder, 4.5×10^{-3} cm^3. With an average density of polyimide films of 1.3g/cm^3,[29] the surface mass interrogated by XPS would be approximately 1.3×10^{-6} g. Using fluorine atomic weight and the fact that each AEFO molecule has approximately 60 F atoms, $\phi(x)$ was determined at each loading level. From the starting material masses used to generate each film ϕ_{bulk} was calculated to determine z^*.

Surface excess concentration was determined at each AEFO loading level for the PIAEF$_{60}$ compositions evaluated using XPS (Table IV). As can be seen, after an initial rapid increase the surface excess reached a maximum of approximately 1.3×10^{-6} mol/m^2 at 0.8 wt % AEFO. Additional AEFO did not lead to significant increase in z^*, on average, suggesting that micelle-like bulk aggregation was likely occurring. The ratio of z^* and the bulk concentration calculated for the same interfacial area as z^* were determined (Figure 5). At very low AEFO loading levels, the surface excess concentration was >400 higher than the bulk and rapidly diminished to <100 at an AEFO loading level of 0.8 wt %.

Researchers have used self-consistent field theory (SCFT) to determine the thermodynamic driving force, or sticking energy $\beta k_B T$, of preferentially migrating species in polymer brush systems[31,32] and upon change in surface chemical functionalities[33] among other systems. The sticking energy is offset by an entropic factor for surface segregation. Sticking energy values for surface migration of fluorinated species have been reported from $3k_BT$ in polyethylene matrices[34] to $> 6k_BT$ in polystyrene[35] and polylactide matrices.[36] Although not calculated here, it is anticipated that large $\beta k_B T$ values would be calculated for these systems based on the low loading limits observed for these materials relative to those reported elsewhere. This is further indication that there is an extremely unfavorable interaction between the AEFO oligomers and the polyimide matrices leading to surface migration.

CONCLUSION

The fluorinated oligomers investigated in this work were demonstrated to change the surface properties of the parent imide at relatively low loading levels and surface excess concentrations were determined. This change in surface properties was realized without significantly compromising the desired mechanical properties of the bulk matrix. Independent control of surface and bulk properties in these copolymer systems enables these materials to be tailored for a variety of applications.

ACKNOWLEDGMENTS

The authors thank Dr. Everett Carpenter and Dmitry Pestov from Virginia Commonwealth University for XPS measurements and data processing as well as Dr. Jeffrey Hinkley from NASA Langley Research Center for scientific discussion and guidance. This work was funded by the NASA Langley Creativity and Innovation fund.

REFERENCES

1. Lopez-Donaire, M. L.; Santerre, J. P. *J. Appl. Polym. Sci.* **2014**, *131*, 40328.

2. Zhang, W.; Zheng, Y.; Orsini, L.; Morelli, A.; Galli, G.; Chielleni, E.; Carpenter, E. E.; Wynne, K. J. *Langmuir* **2010**, *26*, 5848.
3. Wohl, C. J.; Belcher, M. A.; Ghose, S.; Connell, J. W. *Appl. Surf. Sci.* **2009**, *255*, 8135.
4. Connell, J. *High Perform. Polym.* **2000**, *12*, 43.
5. Tiwari, A.; Gupta, M.; Nema, S. *J. Mater. Sci.* **2004**, *39*, 1695.
6. Xiong, J.; Xia, L.; Shentu, B.; Weng, Z. *J. Appl. Polym. Sci.* **2014**, *131*, 39812.
7. Khayet, M.; Suk, D. E.; Narbaitz, R. M.; Santerre, J. P.; Matsuura, T. *J. Appl. Polym. Sci.* **2003**, *89*, 2902.
8. Tang, Y. W.; Santerre, J. P.; Labow, R. S.; Taylor, D. G. *J. Appl. Polym. Sci.* **1996**, *62*, 1133.
9. Rahman, M. M.; Lee, I.; Chun, H.-H.; Kim, H. D.; Park, H. *J. Appl. Polym. Sci.* **2014**, *131*, 39905.
10. An, Q.; Xu, W.; Hao, L.; Huang, L. *J. Appl. Polym. Sci.* **2013**, *127*, 1519.
11. Kawakami, Y.; Takahashi, K.; Hibino, H. *Macromolecules* **1991**, *24*, 4531.
12. Desai, H.; Cunliffe, A. V.; Stewart, M. J.; Amass, A. J. *Polymer* **1993**, *34*, 642.
13. Giesy, J. P.; Kannan, K. *Environ. Sci. Technol.* **2001**, *35*, 1339.
14. Ellis, D. A.; Mabury, S. A.; Martin, J. W.; Muir, D. C. G. *Nature* **2001**, *412*, 321.
15. Wynne, K.; Makal, U.; Kurt, P.; Gamble, L. *Langmuir* **2007**, *23*, 10573.
16. Fujiwara, T.; Wynne, K. *Macromolecules* **2004**, *37*, 8491.
17. Makal, U.; Wynne, K. *Langmuir* **2005**, *21*, 3742.
18. Chung, J.-S.; Kim, B. G.; Sohn, E.-H.; Lee, J.-C. *Macromolecules* **2010**, *43*, 10481.
19. Kausch, C. M.; Leising, J. E.; Medsker, R. E.; Russell, V. M.; Thomas, R. R. *Langmuir* **2002**, *18*, 5933.
20. Mittal, K. L. Polyimides And Other High Temperature Polymers; Mittal, K. L., Ed.; VSP/Brill: Leiden, The Netherlands, **2009**; Vol. *5*.
21. Collier, F. S., Jr. Overview of ERA Technologies and N+2 Integrated Vehicle Concepts. In AIAA 50th Aerospace Sciences Meeting, Nashville, TN, **2012**.
22. Joslin, R. Overview of Laminar Flow Control. National Aeronautics and Space Administration, **1998**, NASA/TP-1998-208705.
23. Joslin, R. *Ann. Rev. Fluid Mech.* **1998**, *30*, 1.
24. Young, T.; Humphreys, B. *Proc. Instn. Mech. Eng. G. J. Aerospace Eng.* **2004**, *218*, 267.
25. Luftmann, H.; Rabani, G.; Kraft, A. *Macromolecules* **2003**, *36*, 6316.
26. PolyFox Reactive Polymer Intermediates. Available at:http://www.omnova.com/products/chemicals/documents/PolyFox-ReactivePolymerIntermediatesJune2011.pdf. Accessed on May 1, 2014.
27. Wohl, C. J.; Atkins, B. M.; Belcher, M. A.; Connell, J. W. *High Perform. Polym.* **2012**, *24*, 40.
28. Kochi, M.; Chen, C.; Yokota, R.; Hasegawa, M.; Hergenrother, P. M. *High Perform. Polym.* **2005**, *17*, 335.
29. Polyimides. Wilson, D.; Stenzenberger, H. D.; Hergenrother, P. M. Eds.; Chapman and Hall: New York, **1990**; p 297.
30. Chan, C.-M. Polymer Surface Modification and Characterization; Carl Hanser Verlag: Munich, **1994**.
31. Jones, R. A. L.; Norton, L. J.; Shull, K. R.; Kramer, E. J.; Felcher, G. P.; Karin, A.; Fetters, L. J. *Macromolecules* **1992**, *25*, 2359.
32. Shull, K. R. *Macromolecules* **1996**, *29*, 2659.
33. Thompson, R. L.; Hardman, S. J.; Hutchings, L. R.; Narrainen, A. P.; Dalgliesh, R. M. *Langmuir* **2009**, *25*, 3184.
34. Hardman, S. J.; Hutchings, L. R.; Clarke, N.; Kimani, S., M.; Mears, L. L. E.; Smith, E. F.; Webster, J. R. P.; Thompson, R. L. *Langmuir* **2012**, *28*, 5125.
35. Ansari, I. A.; Clarke, N.; Hutchings, L. R.; Narrainen, A. P.; Terry, A. E.; Thompson, R. L.; Webster, J. R. P. *Langmuir* **2007**, *23*, 4405.
36. Hutchings, L. R.; Narrainen, A. P.; Eggleston, S. M.; Clarke, N.; Thompson, R. L. *Polymer* **2006**, *47*, 8116.